RUBBER COVERED ROLLS— THE THERMOVISCOELASTIC PROBLEM A FINITE ELEMENT SOLUTION

R. C. BATRA

University of Missouri–Rolla, Rolla, Missouri, U.S.A

M. LEVINSON

McMaster University, Hamilton, Ontario, Canada

ERIC BETZ

University of Newcastle, New South Wales, Australia

SUMMARY

The coupled thermomechanical behaviour of a layer of thermorheologically simple material bonded to a uniformly rotating rigid cylinder and indented by another rigid cylinder is studied by the finite element method. The various approximations necessary to reduce the problem to one of tractable size and the computational methods used are discussed in some detail. The complete thermal, deformation and stress fields may be computed. Some results, computed for a grid using 'rectangular' elements, presented graphically include the temperature distribution, the stress distribution near the bond surface, the contact pressure distribution and the asymmetric surface deformation of the rubberlike layer.

INTRODUCTION

In this paper we study the problem of the indentation, by a rigid cylinder, of a thermoviscoelastic layer bonded to a uniformly rotating rigid cylinder. Such a situation occurs in various industrial settings, e.g. the paper and pulp industry where both cylinders are of comparable diameters. Other industrial applications may involve quite different geometries. The approach presented here is applicable to all possible geometries. A schematic diagram of the system studied is shown in Figure 1. We assume that sufficient time has elapsed since the start up of the operation for the transient effects to become negligible and consequently we study the steady-state problem where the rubber-like layer has a constant angular velocity of Ω revolutions per sec.

We briefly review the earlier work done on other aspects of the present problem. The analytic elastostatic[1,2] and elastodynamic[3] studies as well as the elastostatic numerical[4] studies show that stresses at the bond surface decay to nearly zero values at points far from the contact region. In addition, the effects of the frictional force at the contact surface, for moderate values of the coefficient of friction, are not significant.[2] Furthermore, dynamic forces do not cause any asymmetry in the deformation[3] and numerical calculations, not included in Reference 3, show that the effect of these forces on the stress distribution is negligible for practical geometries and angular velocities.

Whereas analytical methods are available to solve linear elastic problems, as has been noted by Lynch,[5] such methods are hardly existent for viscoelastic boundary value problems in which the boundary surface where surface tractions are prescribed is not a material surface. Accordingly one, in general, must resort to numerical approaches such as the finite element method. Lynch's study[5] of another steady-state dynamic (homothermal) viscoelastic contact problem shows that the finite element method provides results which agree well with experimental findings. Lynch's work leads one to believe that the finite element method should be applicable to the thermo-viscoelastic problem studied herein.
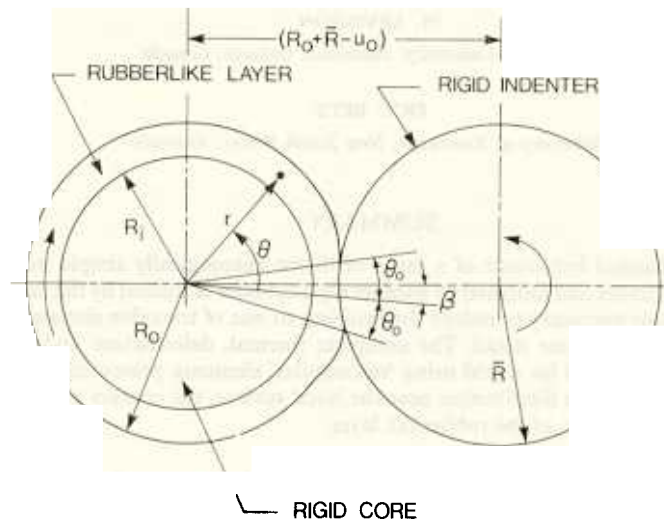

Figure   System to be studied

A difference between the cold rolling problem solved by Lynch and the title problem is the following: whereas in the present case a material particle is subjected to cyclic loading, this is not so for the cold rolling problem. If the material of the covering layer were of a constitutive nature such that the material particle has not recovered completely from the effects of the previous deformation before being subjected to the next loading cycle, then there might be a gradual build up of stresses (as opposed to a cyclic stress pattern) and quite likely the rolls would not last as long as they do in practice. This suggests that the relaxation time of the material of the covering layer is such that at the roll operating speeds currently used, a material particle recovers fully from the effects of the previous deformation before being subjected to the next loading cycle. This observation serves an important role in the development of a numerical solution of the problem studied in this paper.

To ensure that the finite element method will give reasonable results for the present problem, we first solved a homothermal viscoelastic problem.[6] The results obtained were in qualitative agreement with those of Lynch.[5] In view of the fact that no experimental results are available for the problem at hand we were encouraged by the above noted qualitative agreement to proceed with the study of the thermomechanical problem presented in the present paper.

We note that familiarity with the contents of References 1–6, though helpful, is far from essential for an understanding of the work reported below.

FORMULATION OF THE PROBLEM

In the absence of any body forces and external supply of internal energy, the balance laws governing the thermomechanical deformations of the rubber-like layer are[7-9]

$$\sigma_{ij,j} = \rho \ddot{x}_i$$

$$\rho \dot{e} = -q_{i,i} + \sigma_{ij} v_{i,j} \tag{1}$$

Here σ_{ij} is the Cauchy-stress tensor, ρ is the current mass density, x_i is the present position of a material particle X at time t, a superposed dot denotes material time derivative, e is the specific internal energy, q_i is the heat flux per unit surface area in the present configuration, v_i is the velocity of a material particle and a comma followed by an index j indicates partial differentiation with respect to x_j. Throughout this paper we use rectangular Cartesian co-ordinates to describe the deformation of the layer. The last term on the right-hand side of $(1)_2$ represents the work done by the internal stresses per unit time. For viscoelastic materials this term includes the energy dissipated because of viscous dissipation (see, for example, Christensen[9]).

We assume that the deformations of the roll cover are sufficiently small so that we can use constitutive equations linear in the strains. Since the relaxation functions of rubber-like materials are highly temperature-dependent, we will retain the dependence of these functions upon temperature T even though in a strictly linear theory one should assume that the relaxation functions are calculated at the reference temperature T_0. We thus make the following constitutive assumptions for σ_{ij} and q_{ij}.

$$\sigma_{ij}(X, t) = \int_{t-t^*}^{t} G1(T, t-\tau) \frac{\partial \varepsilon_{ij}(X, \tau)}{\partial \tau} d\tau$$

$$+ \frac{\delta_{ij}}{3} \int_{t-t^*}^{t} \{G2 - G1(T, t-\tau)\} \frac{\partial \varepsilon_{kk}}{\partial \tau}(X, \tau) d\tau + \alpha G2, \tag{2}$$

$$q_i = -k T_{,i}$$

Here α is the (constant) coefficient of thermal expansion, k is the (constant) thermal conductivity, ε_{ij} is the infinitesimal strain tensor, t^* is some small fraction of the time period of revolution and $G1$ and $G2$ are, respectively, the shear and bulk moduli. We assume that the bulk behaviour is elastic so that $G2$ is independent of time. We remark that such an assumption is not uncommon for rubber-like materials.[10] If either viscoelastic bulk behaviour is to be considered or the dependence of $G2$ upon the temperature T is to be accounted for, only minor modifications of the subsequent analysis and computational algorithm developed need be made. For reasons stated below we do not need an explicit constitutive equation for e. If required, one should assume a constitutive equation for e which is compatible with (2) and the second law of thermodynamics e.g. see Christensen.[9] Substitution of (2) and a constitutive equation for e into (1) yields field equations for x and T. These field equations need to be supplemented by side conditions such as boundary conditions.

We study here a steady state rotational problem and neglect the effect of *all dynamic* forces. Thus the only side conditions needed are the boundary conditions which may be stated as follows. At the inner surface, $u = x - X = 0$ and at the outer surface,

$$e_i \sigma_{ij} n_j = 0,$$

$$n_i \sigma_{ij} n_j = 0, |\theta| > \theta_0,$$

$$u_i n_i = -u_0 + \frac{R_0}{2}\left(1 + \frac{R_0}{R}\right)(\theta - \beta)^2, \quad |\theta| < \theta_0, \tag{3}$$

$$n_i \sigma_{ij} n_j \to 0 \quad \text{as} \quad |\theta| \to \theta_0$$

Here n_i is an outward unit normal vector to the outer surface and e_i is a unit tangent vector. The right-hand side of (3)$_3$ approximates, within the assumptions of the linear theory, the radial displacement of the outer surface of the bonded layer. In this equation u_0 is the indentation, β is the offset angle, R_0 is the outer radius of the layer, $\bar{R}$ is the radius of the rigid indentor and θ_0 is the semi arc of contact. (3)$_4$ states that the radial stress is continuous across the arc of contact and ensures that a contact problem rather than a punch problem is solved. Of the three unknowns u_0, θ_0 and β appearing in (3)$_3$ at most one can be assumed to be known and the other two are to be determined as a part of the solution.

For the thermal boundary conditions, we take

$$T = T_{\text{inn}} \text{ at the inner surface of the layer}$$

and   (4)

$$T = T_{\text{out}} \text{ at the outer surface of the layer}$$

It is thus tacitly assumed that the rigid core is maintained at the constant temperature equal to that of the inner surface of the covering layer and that the temperature is continuous across the bond surface. If the core were not maintained at a constant temperature, then an appropriate boundary condition would be that the normal component of the heat flux be continuous across the bond surface. This would require a study of the thermal problem for the core. One could approximate the effect of heat conduction in the core by means of a boundary condition of the type suggested by Batra.[11] Similarly, at the outer surface, an alternative boundary condition might be that of mixed type, i.e. either (4)$_2$ or forced convection at the free surface and prescribed heat flux at the contact surface. Since a material particle is in contact with the indentor for a very small fraction of the time of revolution, (4)$_2$ or a boundary condition of the forced convection type on the whole surface would seem to be a good approximation.

The problem as stated above is difficult to solve even numerically. We now make another assumption which though not strictly valid is quite reasonable for the problem at hand. We assume that the layer deforms isothermally, i.e. the temperature of each material point remains constant in time. Note that the temperature of different material points need not be the same. This assumption is equivalent to the assertion that, in cylindrical co-ordinates, the temperature field for our problem is a function of the radius alone. The physical basis for this assumption is as follows. Since heat conduction is a slow process compared to the period of revolution of the rolls the temperature of a material point will vary little during one cycle from its mean value during that cycle. In addition, after a sufficiently long start-up period the mean value of the temperature at a material point will be constant.

Because of the preceding assumption and (2)$_2$, integration of (1)$_2$ over a complete cycle yields

$$\frac{\mathrm{d}^2 T}{\mathrm{d}r^2} = -\frac{1}{Jkt_p} \int_0^2 \text{trace} \, (\boldsymbol{\sigma} \, \text{grad} \, \underline{v}) \, \mathrm{d}\theta = -s^*(r) \tag{5}$$

where J is Joule's constant, t_p is the period of revolution and we have now written (1)$_2$ in cylindrical co-ordinates. It is because of the above assumption that we did not need a specific constitutive equation for e. In (5) s^* is just a function of the radial co-ordinate r. Thus the thermal problem has been reduced to that of solving (5) subjected to the boundary conditions (4). In passing we note that for an elastic layer s^* is identically zero but it is non-negative when the layer is viscoelastic.

Method of solution of the problem

The problem stated above is solved by the following iterative procedure. We first assume an expression such as a fourth order polynomial in r for $s^*(r)$ and solve the thermal problem defined

by (5) and (4) next computing the associated thermal stresses assuming that there are no externally applied mechanical loads. Now, taking the thermally deformed state as the reference configuration and the thermal stresses as initial stresses we solve the mechanical indentation problem wherein we assume that a plane strain state of deformation prevails and properly account for the dependence of the shear modulus on temperature. Then the solution of the mechanical problem is used to compute a new dissipation field which is compared to the assumed one. If these two dissipation fields are sufficiently close to each other, i.e. meet a prescribed tolerance, we consider the problem solved. Otherwise we use the new dissipation field and repeat the calculation until the difference between two consecutively calculated dissipation fields is sufficiently small. In effect, this procedure allows one to solve an intrinsically non-linear problem (in temperature) by a sequence of linear computations. Our approach may be considered as an extension of that used by Taylor et al.[12] for somewhat different problems.

THERMAL STRESS ANALYSIS

We choose to discuss this aspect of our work first because of the ordering of the computational scheme outlined in the preceding section. The question of uniqueness of solution is not considered.

When $s^*(r)$ is a fourth order polynomial† in r, i.e.

$$s^*(r) = a_0 + a_1 r + a_2 r^2 + a_3 r^3 + a_4 r^4 ; \tag{6}$$

the solution of (5) under the boundary conditions (4) is

$$T = -\left[a_0 \frac{r^2}{2} + a_1 \frac{r^3}{6} + a_2 \frac{r^4}{12} + a_3 \frac{r^5}{20} + a_4 \frac{r^6}{30} \right] + a_{11} r + a_{12} \tag{7}$$

where

$$a_{11} = (T_{\text{out}} - T_{\text{inn}} - b_1 + b_2)/(R_0 - R_i$$

$$a_{12} = T_{\text{inn}} + b_1 - a_{11} R_i,$$

$$b_1 = \frac{a_0}{2} R_i^2 + a_1 \frac{R_i^3}{6} + a_2 \frac{R_i^4}{12} + a_3 \frac{R_i^5}{20} + a_4 \frac{R_i^6}{30}, \tag{8}$$

$$b_2 = \frac{a_0}{2} R_0^2 + a_1 \frac{R_0^3}{6} + a_{12} \frac{R_0^4}{12} + a_3 \frac{R_0^5}{20} + a_4 \frac{R_0^6}{30}$$

The constants $a_0, \ldots, a_4$ are chosen arbitrarily for the first iteration and may be taken as zeros. For the subsequent iterations these are calculated by the least square method so as to provide a best fit to the values of $s^*(r)$ computed from the immediately preceding iteration.

Once the temperature distribution is known, the thermal stresses are given by a solution of the field equations

$$\tau_{ij,j} = S_{ij,j} - \alpha G 2 T_{,i} = 0 \tag{9}$$

under the boundary conditions

$$S_{ij} n_j - \alpha G 2 n_i = 0, r = R_0,$$

$$\underline{u} = \mathbf{0} \qquad\qquad r = R_i, \tag{10}$$

---

† This choice of $s^*(r)$ is arbitrary and is made just for convenience. If the layer is divided into L circumferential rings a simple choice for $s^*(r)$ would be a polynomial of order $L-1$. However, other choices such as a sum of trigonometric functions are also feasible.

where

$$S_{ij} = G1\left(\varepsilon_{ij} - \frac{\delta_{ij}}{3}\varepsilon_{kk}\right) + G2\frac{\delta_{ij}}{3}\varepsilon_{kk}$$

$$\tau_{ij} = S_{ij} - \alpha G2\delta_{ij}, \tag{11}$$

$$= \frac{1}{2}\left(\frac{\partial u_i}{\partial X_j} + \frac{\partial u_j}{\partial X_i}\right)$$

We take the reference temperature T_0 equal to T_{inn} and also have used the assumption that the layer deforms isothermally in obtaining (9) from $(1)_1$ and $(2)_1$. After having solved the boundary value problem given by (9) and (10), thermal stresses τ_{ij} are calculated from (11).

A comparison of (9) and (10) with equations governing the mechanical deformations of elastic roll covers[3] suggests that the displacement u produced by the temperature field T is the same as the displacement produced by the body force $-\alpha G2T_{,i}$ and the surface tractions $\alpha G2n_i$ distributed over the surface. For further details concerning this see Reference 13, Section 153. Hence the thermal stress problem can be solved by the finite element method in the same way as the purely mechanical problem. We shall discuss the finite element formulation of the thermal stress problem after discussing the finite element formulation of the mechanical problem since this seems more convenient to us.

FINITE ELEMENT FORMULATION OF THE MECHANICAL PROBLEM

Out of practical necessity we limit our study to the (asymmetrical) deformation in that portion of the roll cover which is symmetric about the line joining the centres of the mating cylinders and which extends over an arc about six times the arc in contact with the indenting cylinder. The necessity referred to is the computing capability available† and the justification for our choice of grid size is as follows. Firstly we recall the rapid decay of stresses indicated by the various analytical elastic studies of our problem[1-3] which was replicated to a high degree of accuracy in the finite element elastic study.[4] An even smaller portion of the roll cover was considered in that numerical study than will be used in the present case. Secondly we note that numerical experiments were conducted in connection with the homothermal viscoelastic case[6] which showed that for the region chosen in that case, which is the same portion of the roll cover we consider here, the boundary conditions imposed on the exit end of the grid had little effect on the stress distribution. This region of interest is divided into uniform curvilinear 'rectangles'. Figure 2 shows a typical element and the location of the rectangular Cartesian axes.

Recalling that a plane strain state of deformation is supposed to prevail, we assume that in each element the displacement is given by

$$u_1 = \alpha_1 + \alpha_2 x_1 + \alpha_3 x_3 + \alpha_4 x_1 x_2,$$
$$u_2 = \beta_1 + \beta_2 x_1 + \beta_3 x_2 + \beta_4 x_1 x_2 \tag{12}$$

Solving for the α's and β's in terms of nodal displacements and calculating infinitesimal strain components from the strain-displacement relation $(11)_3$ we obtain

$$\{\varepsilon\} = \{\mathbf{A}\}\{\boldsymbol{\delta}\} \tag{13}$$
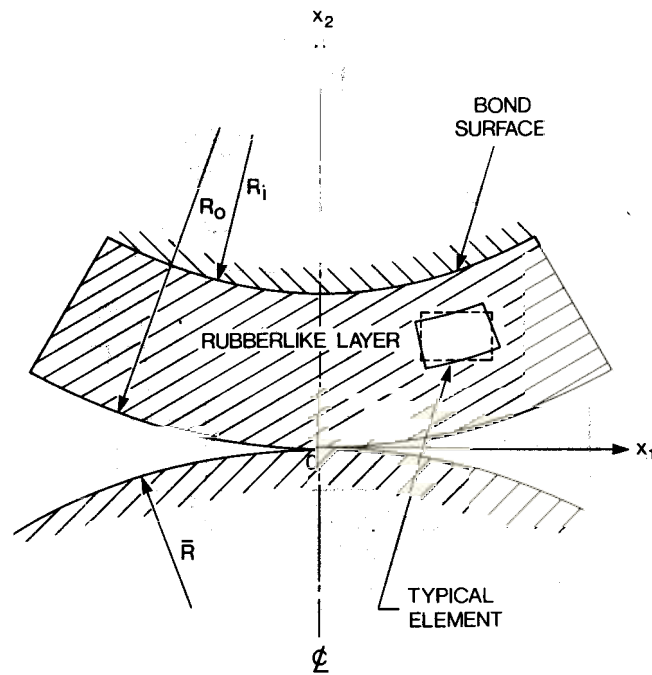
† McMaster University's CDC 6400.

Figure 2. A typical element in the grid

where $\{A\}$ is a 3×8 matrix whose elements are functions of nodal point co-ordinates, $\{\delta\}$ is the vector of displacements of nodal points and $\{\varepsilon\}$ is the vector of strain components. Since a rigid translation of the co-ordinate axes does not affect stresses or strains in an element it is simple to calculate $\{A\}$ for each element with respect to local Cartesian axes $\bar{x}_i$ obtained by translating the origin of the global axes to the centre of the 'rectangular' element. For a typical element, shown in Figure 3,

$$
\{\varepsilon\} \equiv \begin{Bmatrix} \varepsilon_{11} \\ \\ \varepsilon_{22} \\ \\ 2\varepsilon_{12} \end{Bmatrix} = \begin{bmatrix} -\Delta & 0 & \Delta_1 & 0 & \Delta_2 & 0 & -\Delta_2 & 0 \\ \\ 0 & -\Delta_3 & 0 & -\Delta_4 & 0 & \Delta_4 & 0 & \Delta_3 \\ \\ -\Delta_3 & -\Delta_1 & -\Delta_4 & \Delta_1 & \Delta_4 & \Delta_2 & \Delta_3 & -\Delta_2 \end{bmatrix}
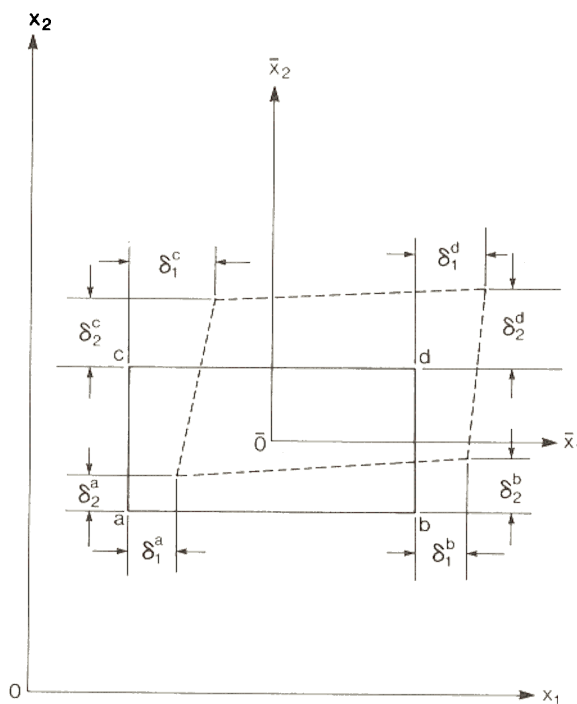$$

Figure 3. Deformation of a typical element

where

$$\Delta_1 = B - \bar{x}_2,$$

$$\Delta_2 = B + \bar{x}_2,$$

$$\Delta_3 = A - \bar{x}_1,$$

$$\Delta_4 = A + \bar{x}_1,$$

and $2A$ and $2B$ are the sides of the 'rectangular' element.

We calculate stresses σ_{ij} is an element from the constitutive relation

$$\sigma_{ij}(\underline{X}, t) = \int_{t-t^*}^{t} \{G2 - G1(T, t-\tau)\} \frac{\partial\{\varepsilon_{kk}(\underline{X}, \tau)\}}{\partial\tau} \, d\tau + \tau_{ij} \tag{15}$$

$$\{\boldsymbol{\sigma}\}_N = \sum_{R=N-M}^{N} \{\mathbf{B}\}_{NR}\{\boldsymbol{\varepsilon}\}_R + \{\boldsymbol{\tau}\}_N, \tag{16}†$$

---

† In (16), and elsewhere $\{\tau\}$ denotes the vector of initial stresses τ_{ij} and is not related to the dummy time variable τ. No confusion should result from this notation.

where

$$\{\sigma\}_N = \left.\begin{array}{c} \sigma_{11} \\ \sigma_{22} \\ \sigma_{12} \end{array}\right\}_N$$

$$\{B\}_{NR} = \left\{\begin{array}{ccc} a_{NR} & b_{NR} & 0 \\ b_{NR} & a_{NR} & 0 \\ 0 & 0 & c_{NR} \end{array}\right\}$$

$$a_{NR} = \left\{\begin{array}{l} -\tfrac{1}{3}\{G1(Y)-G1(Z)\}, \, R \neq N, N-M \\ -\tfrac{1}{3}\{G1(Y)+G1(Z)\}, \, R = N-M, N > M \\ -\tfrac{1}{3}\{G1(0)+G1(\Delta T)\}+\tfrac{1}{3}G2, \, R = N, \end{array}\right.$$

$$Y = (N-R-1)\Delta t$$

$$Z = (N-R+1)\Delta t$$

$$M = t^*/\Delta t$$

Δt = time taken by a material particle to travel from the centroid of one element to the centroid of the next element in the same strip

$$c_{NR} = (b_{NR}-a_{NR})/2$$

and b_{NR} is obtained from a_{NR} by replacing $G1$ by $-\tfrac{1}{2}G1$

The principle of virtual work yields

$$\{F\}_N^T\{\delta\}_N = \int_{V_N} \{\sigma\}_N^T\{\varepsilon\}_N \, dV$$

Substituting from (13) and (16), we obtain

$$\{F\}_N = \sum_{R=N-M}^{N} \{K\}_{NR}\{\delta\}_R + \int_{V_N} \{\varepsilon\}_N^T\{\tau\}_N \, dV \tag{17}$$

where

$$\{K\}_{NR} \equiv \int_{V_N} \{A\}_N^T\{B\}_{NR}\{A\}_R \, dV \tag{18}$$

and $\{F\}_N^T$ is the transpose of the matrix $\{F\}_N$. Here $\{F\}_N$ is the column vector of the forces acting at the nodal points of the element N and V_N is its volume. Equation (17) states that the nodal forces on a typical element N in a control strip are affine functions of the displacements of nodal points associated with all the preceding elements in the same strip. In carrying out the integration in (18) we assume that A and B have the same value for all elements in one strip and, in each element, the mechanical properties are constant and equal their values at the centroid of the element. This results in considerable simplification and, upon carrying out the integration,

we obtain the following for the lower half of the symmetric matrix $\{K\}_{NR}$.

$$[K_{11} = K_{33} = -2K_{51} = K_{55} = K_{77} = -2K_{73}]_{NR} = (a_{NR}b_1 + c_{NR}b_2)/3$$

$$[K_{21} = K_{61} = -K_{52} = K_{74} + K_{65} = -K_{87} = K_{83} = -K_{43}]_{NR} = (b_{NR} + c_{NR})/4$$

$$[K_{31} = K_{75}]_{NR} = (c_{NR}b_2 - 2a_{NR}b_1)/6$$

$$[K_{41} = K_{85} = K_{63} = -K_{81} = -K_{32} = -K_{54} = K_{72} = -K_{76}]_{NR} = (n_{BR} - c_{NR})/4$$

$$[K_{53} = K_{71}]_{NR} = (a_{NR}b_1 - 2c_{NR}b_2)/6$$

$$[K_{44} = K_{22} = -2K_{84} = -2K_{62} = K_{66} = K_{88}]_{NR} = (a_{NR}b_2 + c_{NR}b_1)/3$$

$$[K_{86} = K_{42}]_{NR} = (a_{NR}b_2 - 2c_{NR}b_1)/6$$

$$[K_{64} = K_{82}]_{NR} = (c_{NR}b_1 - 2a_{NR}b_2)/6$$

where

$$B/A, \qquad b_2 = A/B$$

Calculating forces for each element from (17), assembling these for the entire grid, and using the fact that for the entire grid

$$\int \{\tau\}^T \{\varepsilon\} \, dV = \{0\}$$

we obtain

$$\{F\} = \{K\}\{\delta\} \tag{19}$$

where $\{K\}$ is the stiffness matrix for the entire grid, $\{F\}$ is the vector of the nodal forces, and $\{\delta\}$ is the vector representing the displacements of nodal points. Note that $\{K\}$ is not symmetric even though $\{K\}_{NR}$ is symmetric.

Since inertia forces are neglected, (19) is the equation of motion (or equilibrium) which is to be solved together with suitable boundary conditions. To solve (19), we first rewrite it as

$$\begin{Bmatrix} K_{ff} & K_{fb} \\ K_{bf} & K_{bb} \end{Bmatrix} \begin{Bmatrix} \delta_f \\ \delta_b \end{Bmatrix}$$

Here the subscript b signifies a quantity for the nodes on the bond surface where displacements are prescribed and the subscript f signifies a quantity for the remaining nodes. Since

$$\{\delta_b\} = \{0\}$$

it is the following reduced system of equations which must be solved.

$$\{F_f\} = \{K_{ff}\}\{\delta_f\} \tag{20}$$

In order to solve (20) we assume an arc of contact and the distributed load on the contact surface is replaced by a set of concentrated loads at nodal points on the contact surface.† At these nodes only normal forces act and the forces in the tangential direction are taken as zero in order to satisfy the assumed boundary condition of no frictional force at the contact surface.

† Instead of using (3)₃, we are substituting a boundary condition of the surface traction type.

Since the effect of body forces is neglected, $F_f = 0$ except at nodes on the contact surface. The system of equations (20) is solved by the following iterative procedure.

The first step in this iterative scheme is to write $\dot{K}$ as the sum of two matrices[14] i.e. to rewrite (20) as

$$\{F\} = \{K1 + K2\}\{\delta\}$$

where

$$K1_{ij} = \begin{cases} K_{ij}, & |i-j| \leqslant n_b, \quad i = 1, 2, \ldots \\ 0, & |i-j| > n_b \end{cases}$$

$$K2_{ij} = K_{ij} - K1_{ij}$$

Thus $K1$ is a banded matrix of band width $2n_b + 1$. The successive iterations are given by

$$\{\delta\}_n = \{K1\}^{-1}\{F - \{K2\}\{\delta\}_{n-1}\}$$

where

$$\{\delta\}_0 = \{K1\}^{-1}\{F\}$$

and the subscript n signifies the iteration number. Writing (22) as

$$\{\delta\}_n = \left[\sum_{m=0}^{n-1} (-1)^m \{K3\}^{m-1}\right]\{\delta\}_0$$

where

$$\{K3\} = \{K1\}^{-1}\{K2\} \tag{24}$$

we see that a sufficient condition for the convergence of the series on the right-hand side of (23) and hence of the iterative scheme is that

$$\sum_j |K3_{ij}| < 1, \quad i = 1, 2, \ldots \tag{25}$$

This condition serves as a guide to the choice of a value of n_b. A larger value of n_b would, in general, result in a smaller value of the left-hand side of (25) and, therefore, the iterative scheme will converge in fewer iterations. However, a large value of n_b requires more core storage and, therefore, a compromise is sought between how large one can choose n_b and the core storage available. With n_b equal to twice its value for the elastic case, the condition (25) is satisfied since in our case $G1$ is about two orders of magnitude lower than $G2$, the dilation was assumed elastic and the relaxation time is very small. For the case when the bulk behaviour is also viscoelastic or the relaxation time is large (25) may not be satisfied. In such a case, one can use the accelerated Gauss–Seidel iterative method to solve (20) as was done in Reference 6. The iterative procedure (23) is stopped when

$$|[\delta_j^i]_n - [\delta_j^i]_{n-1} < \varepsilon_1, \quad i = 1, 2, 3, \ldots, j = 1, 2 \tag{26}$$

Here ε_1 is a preassigned small positive number. This iterative scheme converged in about 5 iterations for the problem studied here when n_b was set equal to twice its value for the elastic case and $\varepsilon_1 = 10^{-5}$ (this is about 3 orders of magnitude smaller than δ_{max}).

Having solved for the displacements, a check is made to ensure that the assumed arc of contact

† Here we have dropped the subscript f for convenience.

is correct and the deformed surface of the roll cover conforms to, within an acceptable accuracy, the circular profile of the indentor. Should the deformed surface of the roll cover not tally with the shape of the indentor, the loads on the contact surface are adjusted in the manner detailed below and the problem is solved again.

To perform the above-mentioned check and make an adjustment, if necessary, we proceed as follows. First a point $\bar{C}$ is fixed on the line joining the centres of the mating cylinders. The position of $\bar{C}$ is given by

$$(O\bar{C})_j = \frac{1}{m} \sum_{i=n_1+1}^{n_1+m} (OC)_{ji} \qquad (27)$$

where

$$(OC)_{ji} \equiv \{\bar{R}^2 - (x_1^i + (\delta_1^i)_j)^2\}^{\frac{1}{2}} - \{x_2^i + (\delta_2^i)_j\}, \qquad (28)$$

$n_1+1, n_1+2, \ldots, n_1+m$ are the m nodal points which lie on the assumed contact surface, j is the iteration number for the assumed loads, and $\bar{R}$ is the radius of the indentor. In geometrical terms (27) states that if an arc of radius $\bar{R}$ is drawn with $\bar{C}$ as its centre, it would fit well the displaced position of the nodes $n_1+1, n_1+2, \ldots, n_1+m$. Defining the error coefficient e_{ji} by the relation

$$e_{ji} \equiv (OC)_{ji} - (O\bar{C})_j \qquad (29)$$

we consider that the nodes $n_1+1, n_1+2, \ldots, n_1+m$ lie on the rigid indentor, to within an acceptable tolerance, if

$$|e_{ji}| \leqslant \varepsilon_2, \quad i = n_1+1, \ldots, n_1+m \qquad (30)$$

where ε_2 is a suitably chosen small positive number and accept that the assumed arc of contact is correct if

$$e_{ji} \leqslant -\varepsilon_2 \quad \text{for} \quad i = n_1 \quad \text{and} \quad i = n_1+m+1 \qquad (31)$$

If (31) is not satisfied, a new arc of contact is assumed and the whole procedure repeated again. However if (29) holds but (30) does not, then the loads for the next iteration are calculated from the following equation.

$$(F_r^i)_{j+1} = (F_r^i)_j(1 + e_{ji}/\delta_2^{n_1 + [m/2]}) \qquad (32)$$

In (31) $[m/2]$ is the integer obtained by dividing either m or $m+1$ by 2 and F_r^i stands for the radial load at the ith node. The number of iterations required on the nodal load vectors depends strongly on the initial choice of these loads.

The effect of the change in the direction of loads as the contact surface deforms is of an order of magnitude smaller than that retained in a linear theory and is therefore not accounted for herein. If desired, this can be built into the computation scheme without much effort.

To ensure that a contact problem rather than a punch problem has been solved, we verify that the loads vanish as the ends of the arc of contact are approached. We find the arc of contact by plotting the contact pressure and thus satisfy the above condition implicitly.

Having solved the mechanical problem, the value of $s^*(r)$ is calculated from $(5)_2$. Assuming that $\sigma_{ij}\dot{\varepsilon}_{ij}$ is negligible outside the region of interest, an assumption later verified by the numerical results which indicate that the stresses and strains remain constant outside the region of interest, we integrate $(5)_2$ and obtain the following relation

$$s^* = \frac{1}{Jkt_p} \sum_{N=1}^{N^*} \bar{\sigma}_{ij}(N) \, \Delta\varepsilon_{ij}(N)$$

Here s^* is the value of $s^*(r)$ at the centre of a strip, $\bar{\sigma}_{ij}(N)$ is the value of the stresses at the centroid of the Nth element in that strip, $\Delta\varepsilon_{ij}(N)$ equals the value of ε_{ij} at the middle point of the side $\overline{bd}$ of the Nth element (Figure 3) minus the value ε_{ij} at the centre of the side $\overline{ac}$ of the Nth element, and N^* is the total number of elements in a strip.

FINITE ELEMENT FORMULATION OF THE THERMAL STRESS PROBLEM

We proceed, analogous to our approach to the mechanical problem, and use the principle of virtual work to obtain

$$\sum_N \int_{V_N} \tau\}_N^T \{\varepsilon\}_N \, dV = \sum_N \left\{ \int_{V_N} \{S\}_N^T \{\varepsilon\}_N \, dV - \alpha G2 \int_{V_N} (T - T_0)_N \{\varepsilon\}_N \, dV \right\} = \{0\} \qquad (34)$$

or

$$\{K4\}\{\delta\} = \{H\}$$

where

$$\{H\} = \sum_N \{H\}_N \qquad (35)$$

$$\{H\}_N = \alpha G2 \int_{V_N} (T - T_0)\{A\}_N^T \, dV$$

In carrying out the integration in $(35)_2$, we assume that T varies linearly within an element i.e.

$$T - T_0 = T_1 + T_2 X_2$$

We assume this for the sake of simplicity; any other reasonable assumption concerning the variation of T might be used. Note that to integrate the left-hand side of (18) we assumed that $\{B\}_{NR}$ was evaluated at the temperature of the centroid of the element and had the same value throughout the element. This is equivalent to assuming that the temperature in each element remains constant. Since the 'body forces' induced by the temperature variation in the layer depend upon thermal gradients, the assumption that the temperature is constant in each element may not be a good one, at least for a coarse grid, when analysing the thermal stresses. Substituting for $\{A\}_N$ from (14) into $(35)_2$ and simplifying, we obtain

$$\{H\}_N = \begin{Bmatrix} H_1^a \\ H_2^a \\ H_1^b \\ H_2^b \\ \\ H_1^c \\ H_2^c \\ H_1^d \\ H_2^d \end{Bmatrix} = \alpha G2 \begin{Bmatrix} T_2(B^2/3) - T_1 B \\ -AT_1 \\ BT_1 - B^2 T_2/3 \\ -AT_1 \\ \\ BT_1 + T_2 B^2/3 \\ AT_1 \\ -BT_1 - T_2 B^2/3 \\ AT_1 \end{Bmatrix} \qquad (36)$$

$\{K4\}$ in (34) can be obtained from $\{K\}$ in (19) by setting $G1(t) = G1(0)$ in (15). $\{K4\}$ is a symmetric banded matrix and the system of equations (34) can be solved directly. Knowing $\{\delta\}$, strains and hence stresses can be calculated.

COMPUTATION AND DISCUSSION OF RESULTS

We proceed as follows in order to provide some sample results. The region of interest is divided into six curvilinear strips of uniform thickness and each strip is divided into uniform elements by radial lines 0·01 rad apart. The computer program developed computes the stiffness matrix for each element of the grid, assembles the stiffness matrix for the entire grid, solves the system of linear equations by the iterative procedure stated above and, in the mechanical problem, checks whether the profile of the indented surface conforms, within an acceptable accuracy, to that of the indentor and adjusts loads on the contact surface if necessary, computes stresses and strains in each element, the temperature, and the work done per unit volume in each cycle. Then a check is made to determine whether the computed value of s^* is sufficiently close to the assumed one. The program is documented in an internal report which is publicly available.[15]

To solve the thermal stress problem, first a value of s^* is assumed in each strip. A fourth order polynomial is fitted to these values by the least square method; this determines the a's in (6). The value of the temperature at the centre of each strip is then calculated from (7). The stiffness matrix and the forces $\{H\}$ due to thermal gradients are computed for each element and assembled for the entire grid. Since the grid used does not span the complete ring, one has to apply forces at the ends of the grid equal to those exerted on it by the remaining portion of the ring. The system of linear equations (34) is solved for the displacements and the stresses at the centroids of the elements are computed from $(11)_2$.

Since the temperature is assumed to vary radially only, one would expect that the thermal stresses are functions of the radius alone. However, the numerical results computed by the above procedure indicate that the thermal stresses are not the same for all elements in one strip. This variation in the value of the stresses in the elements close to the edges of the grid can be explained by Saint Venant's Principle[13] since we are replacing the exact distribution of forces at the ends of the grid by an approximate discrete one. One can overcome this problem by solving the thermal problem for the entire ring. However, in the results presented below, we assumed that thermal stresses in a strip are the same as those in an element at the middle of the strip.

For our sample case we took the following values for the various parameters

$$
\left.
\begin{aligned}
G1(t) &= 33557(1 + e^{-t/\lambda(T)}) \text{ lb/in}^2 \\
G2 &= 5 \times 10^6 \text{ lb/in}^2 \\
R_0 &= \bar{R} = 18 \text{ in}, \quad R_i = 17 \cdot 5 \text{ in} \\
\Omega &= 4 \text{ rev/sec} \\
\alpha &= 10^{-4}/^\circ\text{F} \\
k &= 0 \cdot 135 \text{ BTU/hr ft}^\circ\text{F} \\
\varepsilon_1 &= 10^{-5} \\
\lambda(T) &= 0 \cdot 01/f(T) \\
\log_{10} f(T) &= \frac{8 \cdot 86(T - T_{\text{inn}})/1 \cdot 8}{101 \cdot 6 + (T - T_{\text{inn}})/1 \cdot 8}
\end{aligned}
\right\}
\tag{37}
$$

and the solution of the problem was assumed to converge when the current calculated value of s^* was within one per cent of the preceding value. In $(37)_4$, $\bar{R}$ is the radius of the indentor. The assumptions $(37)_{1,10,11}$ imply that the material is thermorheologically simple[15] and equations $(37)_{10,11}$ relating the relaxation time $\lambda(T)$ at temperature T (°F) to the relaxation time $\lambda(T_{\text{inn}}) =$

0·01 at the reference temperature T_{inn} (°F) constitute the WLF equation.[16] In $(37)_{11}$ the factor 1·8 is the conversion factor from °F to °C and the reference temperature is taken equal to T_{inn} for convenience. Usually it is taken equal, in degrees Celsius, to the glass transition temperature of the material plus 50.[16] Here we have assumed that $G1(0)$ and $G2$ do not depend upon temperature. The former is consistent with the assumption of a thermorheologically simple material. The dependence of $G1(0)$ and $G2$ upon T can easily be incorporated into the analysis and the computer program. Figure 4 shows how $G1(t)$ varies with the temperature in our case.
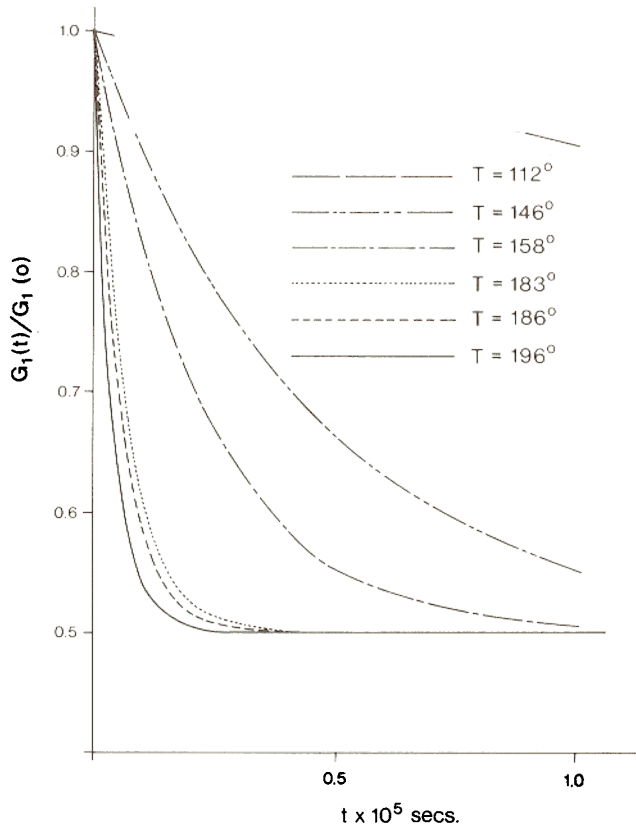

Figure 4. Variation of shear modulus with temperature

To compute the results, we first used a grid with 24 elements in each strip and assumed that $t^* = 24\Delta t$. The resulting temperature distribution showed that the relaxation time of the material points in each strip was extremely small so that the material 'forgot', almost instantaneously, what happened to it in the past. We then computed results for the grid with 24 elements in each strip but taking $t^* = 10\Delta t$ and found that the two sets of results were nearly identical. Because of the lower value of t^*, we could compute results for a grid with 36 elements in each strip and this grid is used henceforth.

The results presented below are for the case when the exit end of the grid is assumed free. Because the grid is coarse, numerical results may not be very accurate. A finer mesh could not be used because of the limited core storage available in the CDC 6400 computer at McMaster University.

In Figure 4, we have plotted $G1$ as a function of t at the temperatures of the centres of various strips. Figure 5 shows the temperature distribution across the thickness of the layer. Since $G1$ has the same value for all points in one strip, we may view the roll cover as being made of various homogeneous isotropic layers having different mechanical properties.
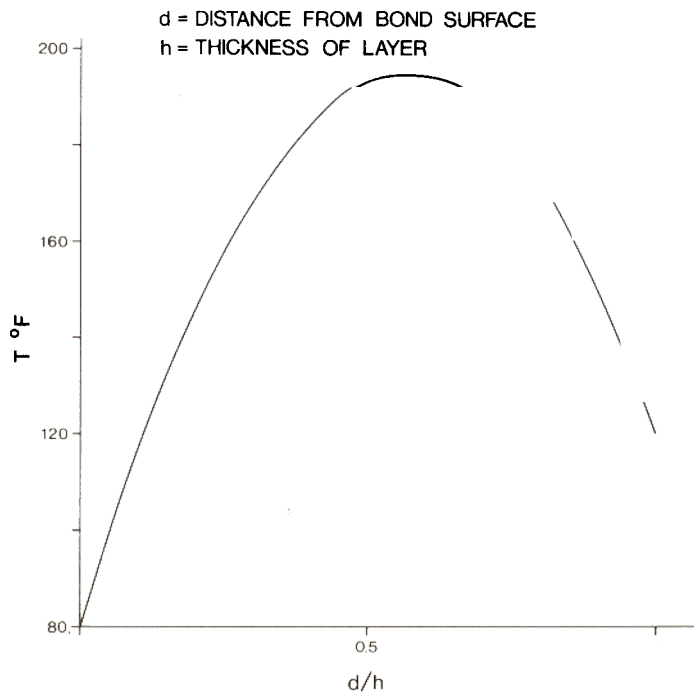
Figure 5. Temperature distribution across the rubber-like layer

Figures 6, 7 and 8 show that the deformed surface of the roll cover, the pressure distribution at the contact surface, and stresses near the bond surface are all symmetric about the line joining the centres of the mating cylinders. These results, due to viscoelastic dissipation, are in qualitative agreement with those obtained earlier for the homothermal viscoelastic problem.[6] Strains computed from (14) indicated that the maximum strain occurred near the centre of the strip and was approximately equal to 0·027. It is possible that for the sample calculation given here we may have reached the limit of the range of validity of the linear theory. The elastic load distribution shown in Figure 7 was obtained from the thermoviscoelastic program by taking

$$G1(t) = 67114 \, \text{lb/in}^2$$

$$G2(t) = 5 \times 10^6 \, \text{lb/in}^2$$

$$\tau_{ij} = 0$$

in the constitutive relation (15) and the semi-arc of contact $\theta_0 = 0\cdot02$. Whereas in this elastic case the arc of contact originated and terminated at a nodal point it was not so for the thermoviscoelastic problem. In that case the boundaries of the arc of contact were located graphically
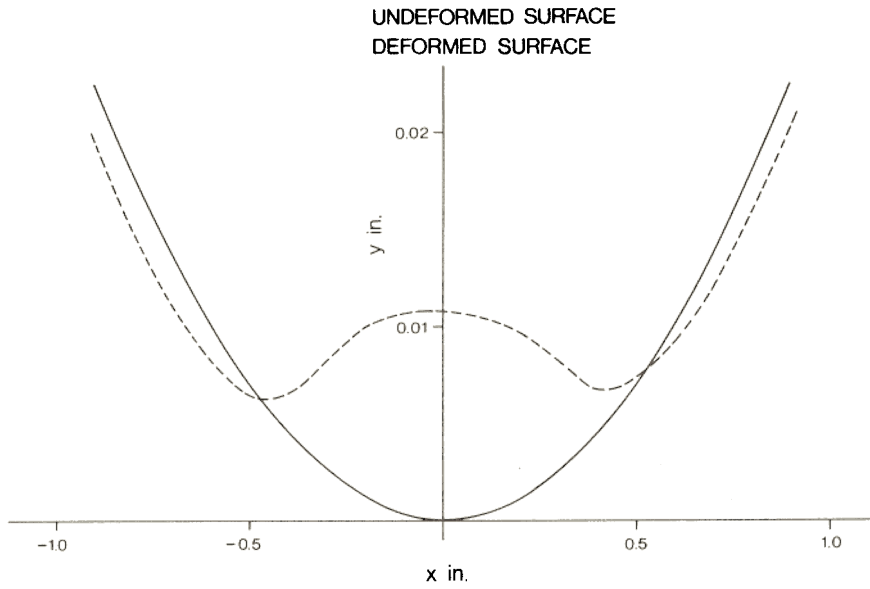
UNDEFORMED SURFACE
DEFORMED SURFACE

Figure 6. Asymmetric surface deformation of the rubber-like layer

ELASTIC CASE

THERMOVISCOELASTIC CASE

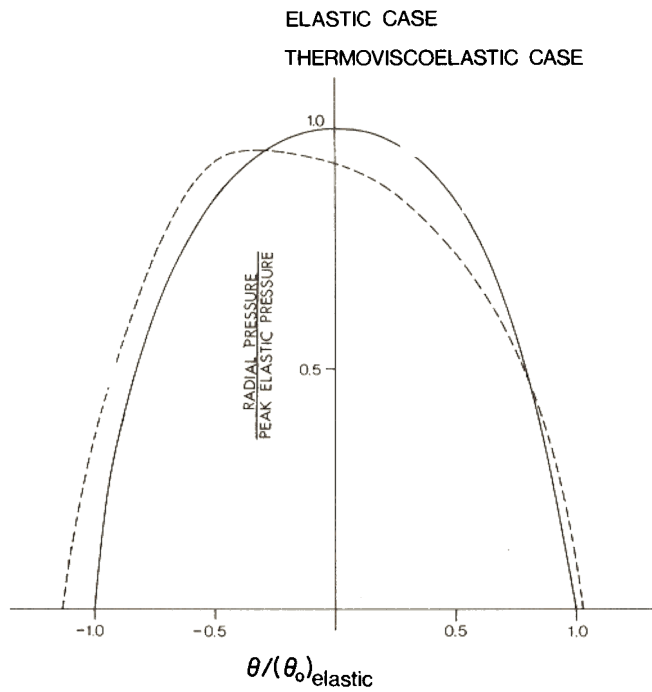$\dfrac{\theta}{(\theta_o)}_{\text{elastic}}$

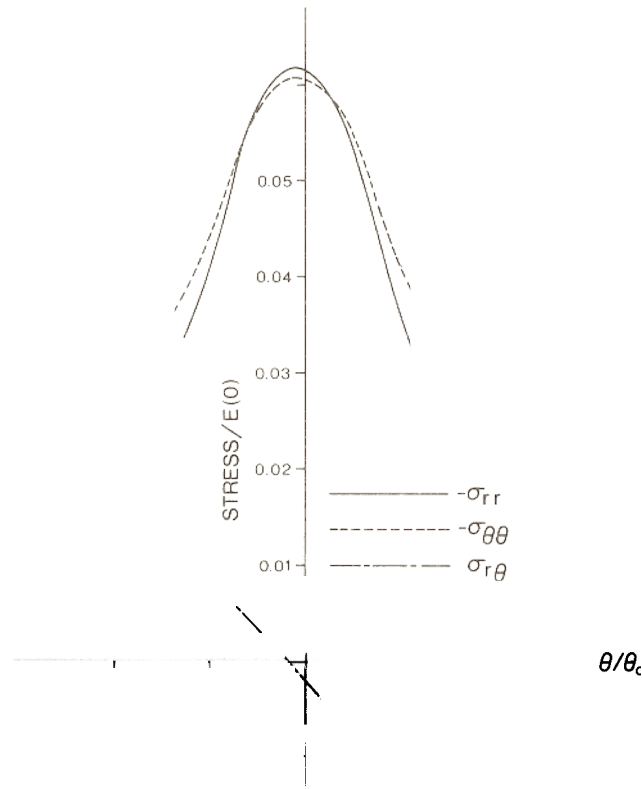Figure 7. Comparison of thermoviscoelastic and elastic contact pressure distributions

Figure 8. Stress distribution near the bond surface

by plotting the load distribution and there the value of θ_0 was found to be 0·215. However, this was checked by ensuring that nodal points beyond both ends of the arc of contact indeed were neither on the contact surface nor penetrating the indentor.

It is clear from the pressure distribution shown in Figure 7 that the force distribution at the contact surface gives a moment which opposes the motion of the layer. Thus to keep the system running at a steady speed work has to be done on the system. For the values of various parameters given in (37), the power required to maintain the system in steady state rotation is 5.17 HP per linear inch of the roll. For our case this is equivalent to a coefficient of friction approximately equal to 0·03 acting between the rolls.

A comparison of the results obtained here using the 'rectangular' element and those obtained in Reference 6 using triangular elements shows that the present mesh with rectangular elements gives considerably better results. One could further improve the accuracy of the results by computing the stiffness matrix on the assumption that the temperature varies linearly or in some other more complicated fashion across the element.

Here we have not accounted for the frictional force at the contact surface. One can account for this easily by applying appropriate tangential forces at the nodal points on the contact surface. For example, if one assumes Coulomb friction with impending slip everywhere on the contact surface[2] one can specify the tangential force at a nodal point to be equal to the coefficient of friction multiplied by the normal force and proceed to solve the problem in exactly the same fashion as we have done.

We have replaced the force exerted by the indentor by equivalent loads at the nodal points. Sometimes one wishes to replace the actual load distribution by work equivalent loads. This would require a knowledge of the exact arc of contact. Since, in the thermoviscoelastic case and for the mesh used here, it is not feasible to specify the arc of contact precisely, we can not compute the work equivalent loads. However for a sufficiently fine mesh for which the arc of contact originating and terminating at a nodal point can be ascertained *a priori*, one can calculate work equivalent loads and specify these at the nodal points on the contact surface.

Since, in practice, one is more likely to know the total contact force rather than the contact arc, the application of our method to a real problem will involve prior work to estimate the correspondence between total contact force and contact arc. An examination of Figure 7 suggests that a sufficiently accurate estimate may be achieved if the preliminary work is done using an elastic model.

Finally, we note for the interested reader that a paper surveying the paper mill problem and the research strategy which led to the present work was presented at the Second Symposium on the Applications of Solid Mechanics.[17]

ACKNOWLEDGEMENT

REFERENCES

1. H. T. Hahn and M. Levinson, 'Indentation of an elastic layer(s) bonded to a rigid cylinder—I. Quasistatic case without friction', *Int. J. Mech. Sci.* **16**, 489–502 (1974).
2. H. T. Hahn and M. Levinson, 'Indentation of an elastic layer bonded to a rigid cylinder—II. Unidirectional slipping with friction', *Int. J. Mech. Sci.* **16**, 503–514 (1974).
3. R. C. Batra, M. Levinson and H. T. Hahn, 'Extension of an energy theorem of Barenblatt to elastodynamics and its application to a problem of rolling contact', *CEEM Report No. 73–8*, McMaster Univ., Hamilton, Canada (1973).
4. E. Betz and M. Levinson, 'Rubber covered rolls—the elastic problem. A finite element solution', *CEEM Report No. 73–7*, McMaster Univ., Hamilton, Canada (1973).
5. F. de S. Lynch, 'A finite element method of viscoelastic stress analysis with application to rolling contact problems', *Int. J. num. Meth. Engng*, **1**, 379–394 (1969).
6. R. C. Batra, M. Levinson and E. Betz, 'Rubber covered rolls—The isothermal viscoelastic problem. A finite element solution', *CEEM Report No. 74–1*, McMaster Univ., Hamilton, Canada (1974).
7. J. T. Oden, *Finite Elements of Nonlinear Continua*, McGraw-Hill, New York, 1972.
8. T. L. Cost, 'A free energy functional for thermorheologically simple materials', *Acta Mech.*, **17** 153–167 (1973).
9. R. M. Christensen, *Theory of Viscoelasticity—An Introduction*, Academic Press, New York, 1971.
10. L. W. Morland and E. H. Lee, 'Stress analysis for linear viscoelastic materials with temperature variation', *Trans. Soc. Rheology*, **4**, 233–263 (1960).
11. R. C. Batra, 'On non-classical boundary conditions', *Arch. Rat'l Mechs. Anal.*, **48**, 163–191 (1972).
12. R. L. Taylor, K. S. Pister and G. L. Goudreau, 'Thermomechanical analysis of viscoelastic solids', *Int. J. num. Meth. Engng*, **2**, 45–59 (1970).
13. S. P. Timoshenko and J. N. Goodier, *Theory of Elasticity*, 3rd edn., McGraw-Hill, New York, 1970.
14. R. S. Varga, *Matrix Iterative Analysis*, Prentice-Hall, Englewood Cliffs, N.J., 1962.
15. R. C. Batra, M. Levinson and E. Betz, 'Rubber covered rolls—the thermoviscoelastic problem. A finite element solution', *CEEM Report No. 74–2*, McMaster Univ., Hamilton, Canada (1974).
16. J. D. Ferry, *Viscoelastic Properties of Polymers*, Wiley, New York, 1961.
17. M. Levinson, R. C. Batra, E. Betz and H. T. Hahn, 'Paper mill rolls—from elasticity to thermoviscoelasticity', *Proc. 2nd Symp. Appl. Solid Mech.*, McMaster University (1974).